Outbreak of NDM-5-Producing Proteus mirabilis During the COVID-19 Pandemic in an Argentine Hospital

Barbara Ghiglione , Ana Paula Rodriguez , María Sol Haim , Laura Esther Friedman , Nilton Lincopan , María Eugenia Ochiuzzi , José Alejandro Di Conza *

Posted Date: 15 April 2025

doi: 10.20944/preprints202504.1221.v1

Keywords: Proteus mirabilis; ST135; NDM-5; outbreak; RmtB; IncQ plasmid; biofilm formation

 doi:10.20944/preprints202504.1221.v1

Article

Outbreak of NDM-5-Producing *Proteus mirabilis* During the COVID-19 Pandemic in an Argentine Hospital

Barbara Ghiglione [1,2,#], Ana Paula Rodriguez [3,#], María Sol Haim [1,4], Laura Friedman [1], Nilton Lincopan [5], María E. Ochiuzzi [3] and José Di Conza [1,2,*]

[1] Universidad de Buenos Aires, Facultad de Farmacia y Bioquímica, Instituto de Investigaciones en Bacteriología y Virología Molecular (IBaViM), Ciudad Autónoma de Buenos Aires, Argentina; BarbaraGhiglione@gmail.com (BG); solhaim@gmail.com (SH); lauraestherfriedman@gmail.com (LF); jdiconza@gmail.com (JDC)

[2] Consejo Nacional de Investigaciones Científicas y Técnicas (CONICET), Ciudad Autónoma de Buenos Aires, Argentina

[3] Hospital General de Agudos "Carlos G. Durand", Ciudad Autónoma de Buenos Aires, Argentina; rodriguezapaula@gmail.com (APR); eugeoc@gmail.com (MEO)

[4] Unidad Operativa Centro Nacional de Genómica y Bioinformática, ANLIS Dr. Carlos G. Malbrán, Ciudad Autónoma de Buenos Aires, 1282, Argentina

[5] Department of Microbiology, Instituto de Ciencias Biomedicas, Universidade de Sao Paulo, Sao Paulo, Brazil; lincopan@usp.br (NL)

* Correspondence: jdiconza@gmail.com; Tel.: +54-11-5287-4804

[#] These authors contributed equally to this work.

Abstract: During the COVID-19 pandemic, the emergence of multidrug-resistant (MDR) pathogens, driven by heightened antibiotic usage and device-associated infections, has posed significant challenges to healthcare. This study reports an outbreak of *Proteus mirabilis* producing NDM-5 and CTX-M-15 β-lactamases in a hospital in Buenos Aires, Argentina, from October 2020 to April 2021. To our knowledge, this represents the first documented outbreak of NDM-5-producing *P. mirabilis* in the country. Eighty-two isolates were recovered from 40 patients, 41.5% from blood cultures and 18.3% from respiratory and urinary samples, among others. Most isolates exhibited resistance to carbapenems, cephalosporins, aminoglycosides, and fluoroquinolones, while retaining susceptibility to aztreonam. Genetic analysis confirmed the co-presence of the $bla_{\text{NDM-5}}$ and $bla_{\text{CTX-M-15}}$ genes, with clonal relationships supported by PCR-based methods and MALDI-TOF MS cluster analysis. Whole-genome sequencing revealed a resistome comprising 25 resistance genes, including *rmtB* and both β-lactamases, as well as the presence of an incomplete IncQ1 replicon associated with multiple resistance determinants. MLST analysis classified this clone as belonging to ST135. Despite the biofilm-forming capacity observed across strains, rifampicin demonstrated potential for disrupting established biofilms at concentrations ≥32 μg/mL in vitro. However, the MDR profile of the outbreak strain significantly limited therapeutic options. The absence of surveillance cultures for the index case limits insights into the outbreak's origin. This study highlights the growing threat of NDM-producing *P. mirabilis* in Argentina and underscores the importance of integrating genomic surveillance into infection control protocols to mitigate the spread of MDR pathogens.

Keywords: *Proteus mirabilis*; ST135; NDM-5; outbreak; RmtB; IncQ plasmid; biofilm formation

1. Introduction

Proteus mirabilis, a member of the *Enterobacterales* order, exhibits a widespread presence in both natural environments and the gastrointestinal tracts of humans and animals [1]. It is considered an

 doi:10.20944/preprints202504.1221.v1

opportunistic pathogen capable of causing nosocomial infections particularly of the urinary tract, wounds, respiratory tract, catheter related infections and, less frequently, blood [2].

P. mirabilis naturally exhibits resistance to polymyxins, tetracyclines, and tigecycline. Thereby, the acquisition of resistance genes against other antibiotic families as β-lactams, aminoglycosides, fluoroquinolones, becomes a therapeutic challenge [3].

Beyond its role in acute infections, *P. mirabilis* exhibits a remarkable ability to form biofilms. Biofilm formation significantly enhances the bacterium's resistance to antimicrobial agents and host immune responses, making infections caused by *P. mirabilis* challenging to treat. In the healthcare setting, biofilm-related infections are of particular concern, as they contribute to prolonged hospital stays, increased healthcare costs, and higher morbidity rates [4].

Moreover, *P. mirabilis* is able of producing urease leading to increased urine alkalinity and the formation of crystalline biofilms. These biofilms often result in encrustation of medical devices and the development of struvite and apatite stones, further complicating clinical management [5]. The presence of *P. mirabilis* biofilms on catheters poses significant clinical challenges. Catheter encrustation and blockage necessitate frequent replacements, increasing patient discomfort and healthcare costs. Furthermore, biofilm-associated bacteria can serve as a persistent source of infection, potentially leading to severe complications such as pyelonephritis and septicemia.

During the COVID-19 pandemic, the emergence of extremely resistant microorganisms was largely observed and an increase in carbapenem resistance incidence was also documented, possibly linked to the heightened use of broad-spectrum antibiotics in the treatment of COVID-19 patients [6]. Concurrently, there has been an observed rise in the rate of device-associated infections in intensive care units, mainly in central vascular catheters and mechanical ventilation.

In recent years, there has been a significant increase in the prevalence of carbapenem-resistant *Enterobacterales*, with *P. mirabilis* isolates emerging as a particularly challenging concern within clinical environments [7]. This trend has significantly restricted the range of effective therapeutic strategies available. Resistance to carbapenems is mostly mediated through production of carbapenemases such as KPC-2 and NDM-1 [8,9], although to a lesser extent, enzymes such as VIM or IMP contribute to this resistance phenotype [10].

Although different species of NDM-producing *Enterobacterales* were reported in Argentina, its documentation in *P. mirabilis* isolates was barely described. The NDM-5 variant was initially detected in an *E. coli* clinical isolate in 2018 and its prevalence has increased to date [11,12].

Here we describe a short-term hospital outbreak caused by a MDR NDM-5-producing *P. mirabilis* clonal strain during the COVID-19 Pandemic in an acute general hospital in Autonomous City of Buenos Aires, Argentina. To the best of our knowledge, this represents the first report of NDM-5-producing *P. mirabilis* in our country and is among the limited outbreaks attributable to carbapenem resistant *P. mirabilis* reported in the literature.

 doi:10.20944/preprints202504.1221.v1

2. Results

2.1. Epidemiological and Clinical Characteristics of the P. mirabilis Outbreak

The outbreak lasted from October 2020 to April 2021 and involved 82 MDR *P. mirabilis* isolates from 40 hospitalized patients. The first strain was isolated on September 29, 2020, from a 61-year-old male patient with bacteremia. The demographic and clinical characteristics of the affected patients are summarized in Table 1. During the outbreak, *P. mirabilis* isolates were recovered from different clinical samples, including blood cultures (n = 34; 41.5%), tracheal aspirates/bronchoalveolar lavage fluid (n = 15; 18.3%), urine cultures (n = 15; 18.3%), catheters (n = 10; 12.2%), retrocultures (n = 5; 6.1%), and miscellaneous materials (n = 3; 3.6%). Surveillance isolates from anal swabs were not included. A total of 46.2% of the isolates were from patients hospitalized for COVID-19, while 26.8% were associated with other pathologies. The remaining patients were admitted for unknown reasons. The mean age was 52 years (range: 34–90 years), with 65% being male and 35% female.

Table 1. Demographic and clinical characteristics of 40 patients involved in the NDM-5-producing *Proteus mirabilis* outbreak.

Patient	Age	Sex	Sample origin*	Date#	Sample source (n)
1	61	M	ICU	29/9/2020	blood culture (1) urine (1)
2	42	M	MCU	1/10/2020	catheter (2) tracheal aspirate (2)
3	52	M	ICU	8/10/2020	catheter (1)
4	45	M	ICU	20/10/2020	urine (1)
5	51	M	ICU	23/10/2020	urine (1) tracheal aspirate (1)
6	37	F	ICU	27/10/2020	catheter (1) blood culture (1)
7	60	M	ICU	30/10/2020	blood culture (2)
8	46	M	ICU	7/11/2020	catheter (1)
9	53	F	ICU	8/11/2020	blood culture (2) tracheal aspirate (2)
10	57	M	ICU	11/11/2020	blood culture (1) tracheal aspirate (1) urine (1)
11	45	M	MCU	22/11/2020	urine (1) blood culture (1) catheter (1)
12	66	F	GER	25/11/2020	blood culture (1)
13	47	F	MCU	25/11/2020	blood culture (1)
14	50	F	ICU	27/11/2020	blood culture (1)
15	53	F	GS	2/12/2020	tracheal aspirate (1) miscellaneous (1)
16	51	M	MCU	5/12/2020	blood culture (1)
17	55	F	MCU	6/12/2020	miscellaneous (1)
18	45	M	MCU	20/12/2020	blood culture (1)
19	57	M	GER	7/1/2021	blood culture (1) urine (2)
20	65	F	ICU	13/1/2021	tracheal aspirate (1)
21	60	M	MCU	17/1/2021	urine (1)
22	43	M	ICU	21/1/2021	urine (1)
23	48	F	ICU	6/2/2021	blood culture (1) catheter (1)
24	90	M	MCU	9/2/2021	miscellaneous (1)
25	45	M	ICU	10/2/2021	urine (1)
26	50	M	ICU	13/2/2021	blood culture (4) retroculture (1) catheter (1)
27	60	F	ICU	5/3/2021	blood culture (2)
28	71	M	MCU	10/3/2021	urine (1)
29	45	M	ICU	12/3/2021	catheter (2)
30	44	F	GS	24/3/2021	blood culture (3) retroculture (2)
31	54	M	ICU	27/3/2021	tracheal aspirate (1) blood culture (2) urine (2)
32	57	M	ICU	14/4/2021	tracheal aspirate (1)
33	64	M	ICU	17/4/2021	blood culture (2) tracheal aspirate (1)

 doi:10.20944/preprints202504.1221.v1

Patient	Age	Sex	Sample origin*	Date#	Sample source (n)
1	61	M	ICU	29/9/2020	blood culture (1) urine (1)
2	42	M	MCU	1/10/2020	catheter (2) tracheal aspirate (2)
3	52	M	ICU	8/10/2020	catheter (1)
4	45	M	ICU	20/10/2020	urine (1)
34	34	F	ICU	18/4/2021	tracheal aspirate (1)
35	56	F	ICU	24/4/2021	blood culture (2) retroculture (2)
36	54	M	MCU	26/4/2021	blood culture (2)
37	52	M	ICU	27/4/2021	tracheal aspirate (1)
38	55	F	ICU	27/4/2021	tracheal aspirate (1)
39	40	M	ICU	29/4/2021	tracheal aspirate (1)
40	51	M	ICU	30/4/2021	blood culture (2) urine (2)

*ICU: Intensive Care Unit; MCU: Medical Clinic Unit; GS: General surgery; GER: Geriatrics. Samples labeled as "Tracheal aspirate" may also include bronchoalveolar lavage fluid. # Date of the first isolate, (n) = number of isolates.

2.2. Antimicrobial Susceptibility Testing (AST) and Carbapenemase Detection

The AST revealed that all 82 isolates were non-susceptible to imipenem (IMI, MIC ≥ 16 mg/L), meropenem (MEM, MIC ≥ 16 mg/L), cefotaxime (CTX, MIC ≥ 64 mg/L), ceftazidime (CAZ, MIC ≥ 64 mg/L), cefepime (FEP, MIC range 8 - ≥ 16 mg/L), piperacillin/tazobactam (PTZ, MIC range 16/4 – ≥ 124/4 mg/L), amikacin (AMK, MIC range 32 - ≥ 64 mg/L), gentamicin (GEN, MIC ≥ 16 mg/L), ciprofloxacin (CIP, MIC ≥ 4 mg/L) and trimethoprim/sulfamethoxazole (TMS, MIC ≥ 4/76 mg/L) but remained susceptible to aztreonam (AZT). Additionally, all *P. mirabilis* isolates displayed positive results for metallo-β-lactamase (MBL) production. Molecular analysis via PCR confirmed the co-occurrence of *bla*$_{NDM}$, encoding a carbapenemase, and *bla*$_{CTX\text{-}M\text{-}G1}$, encoding an extended-spectrum beta-lactamase (ESBL). Subsequent sequencing of selected amplicons identified the presence of *bla*$_{NDM\text{-}5}$ and *bla*$_{CTX\text{-}M\text{-}15}$ variants.

2.3. Clonal Relationship

A subset of 28 isolates (one per patient, randomly selected) were thoroughly examined to investigate the genetic relationship. Our results indicate minimal variation in amplification band profiles when performing REP- and ERIC-PCR, suggesting a close relationship among the strains (Figure S1). Consistent with the REP and ERIC results, most of these isolates (25/28) were grouped into a single MALDI-TOF cluster when a similarity cutoff of 85% was applied (Figure S2).

2.4. Biofilm Formation and Substrate-Specific Growth

A panel of 6 *P. mirabilis* isolates from different sample sources was evaluated for biofilm formation. Quantitative assays demonstrated that all isolates formed moderate biofilms, as evidenced by biomass measurements. The ODs of the 48 h biofilms stained with CV ranged from 0.398 to 0.894 (Figure 1A, Table S1). The data analysis showed no significant statistical differences in biofilm formation among the isolates. Furthermore, biofilm formation ability was assessed on Foley urinary catheter materials, revealing that biofilms were readily established on latex catheters, whereas silicone catheters showed minimal biofilm development (data not shown), highlighting the material-dependent nature of biofilm formation in *P. mirabilis*.

 doi:10.20944/preprints202504.1221.v1

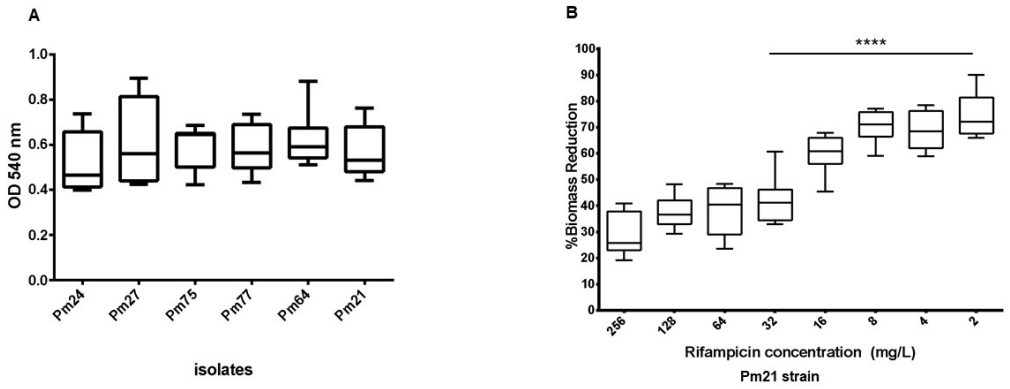

Figure 1. A) Biofilm formation of *P. mirabilis* isolates obtained from different types of samples. B) Effect of rifampicin on biofilm biomass of *P. mirabilis* Pm21 strain. Asterisks (****) indicate $p < 0.0001$ for biomass reduction measurement.

2.5. Impact of Rifampicin on Established Biofilms

The MIC against rifampicin of the six *P. mirabilis* isolates was 16 mg/L. The effect of rifampicin on preformed *P. mirabilis* biofilms was investigated using the microplates model against the Pm21 isolate. Following treatment with rifampicin at concentrations ranging from 256 to 2 mg/l, the minimum biofilm inhibitory concentration (MIC-b) was determined to be 128 mg/L. The minimum regrowth concentration (MRC), the lowest concentration preventing microbial recovery, was ≥256 mg/L. However, biomass quantification after rifampicin exposure revealed a significant reduction starting at 32 mg/L when compared to untreated controls, as confirmed by statistical analysis (Figure 1B, Table S2). These findings underscore the potential of rifampicin to disrupt *P. mirabilis* biofilms, albeit at relatively high concentrations.

2.6. Genome Analysis

Whole-genome sequencing (WGS) analysis of one randomly selected isolate (Pm21) revealed a genome size of 4,265,609 bp, with a GC content of 39.07%, 81 contigs (>1000 bp), and an N50 value of 140,806 bp. Pm21 displayed a multilocus sequence typing (MLST) profile consistent with sequence type (ST) 135 and a virulence profile corresponding to vST138. The resistome analysis predicted multiple acquired antimicrobial resistance genes, including *bla*$_{\text{NDM-5}}$ and *bla*$_{\text{CTX-M-15}}$ (β-lactam resistance), *rmtB*, *aadA1*, *aadA2*, *aadA5*, *aac(3)-IV*, *aac(6')-Ib3*, *ant(3'')-Ia*, *aph(3')-Ia*, *aph(6)-Id* (aminoglycoside resistance), *dfrA1*, *dfrA17*, *dfrA32* (trimethoprim resistance), *sul1* and *sul2* (sulfonamide resistance), *ere(A)* (macrolide resistance), *catA1* (chloramphenicol), and *tet(C)*, *tet(J)* (tetracycline resistance), among others (Table 2). Chromosomal point mutations were not detected since the PointFinder database is curated for species other than *Proteus* sp.

Table 2. Genomic characteristics of Pm21 isolate.

***Proteus mirabilis* Pm21 assembly metrics**	
Characteristics	**Details**
Genome size (bp)	4,265,609
% GC content	39.07
N50 (bp)	140,806
Resistome	

 doi:10.20944/preprints202504.1221.v1

Gene	Predicted Phenotype	%Identity	%Coverage	HSP Length/Total Length
aac(3)-IId	gentamicin	99.88	100	861/861
aac(3)-IV	gentamicin, tobramycin	100	100	777/777
aadA1	streptomycin	100	100	789/789
aadA2	streptomycin	99.88	97,92	802/819
aadA5	streptomycin	99.87	100	789/789
aph(3'')-Ib	streptomycin	100	100	804/804
aph(3')-Ia	kanamycin	100	100	816/816
aph(4)-Ia	hygromycin	100	100	1026/1026
aph(6)-Id	kanamycin	100	100	837/837
***bla*$_{\text{CTX-M-15}}$**	ampicillin, ceftriaxone	100	100	876/876
***bla*$_{\text{NDM-5}}$**	ampicillin, amoxicillin/clavulanic acid, cefoxitin, ceftriaxone, meropenem	100	100	813/813
***bla*$_{\text{OXA-1}}$**	ampicillin	100	100	831/831
***bla*$_{\text{OXA-2}}$**	ampicillin	100	100	828/828
***bla*$_{\text{TEM-1B}}$**	ampicillin	100	100	861/861
cat	chloramphenicol	98.17	100.15	655/654
catA1	chloramphenicol	99.85	100	660/660
catB3	chloramphenicol	100	69.83	442/633
dfrA1	trimethoprim	100	100	474/474
dfrA17-like*	trimethoprim	100	86.92	412/474
dfrA32-like*	trimethoprim	100	86.92	412/474
ere(A)	erythromycin	99.84	100	1221/1221
qacEdelta1	resistance to antiseptics	100	84.68	282/333
rmtB	amikacin, gentamicin, kanamycin, streptomycin	100	100	756/756
sul1	sulfisoxazole	100	100	840/840
sul2	sulfisoxazole	100	100	816/816
tet(C)	tetracycline	99.66	100	1191/1191
tet(J)	tetracycline	99.08	100	1197/1197
Plasmids	IncQ1	100	65.83	524/796
GenBank accession number	Sequence Read Archive submission: PRJNA1236692.			
Genome assembly	https://ri.conicet.gov.ar/handle/11336/252337			

* Located on different contigs in the assembly.

 doi:10.20944/preprints202504.1221.v1

2.7. Genetic Analysis of Resistance Marker Environments

PlasmidFinder identified the IncQ1 replicon type as the only typable plasmid incompatibility group. The IncQ1 replicon was partially detected at the 5′ end of contig 49 (12,303 bp) with 100% identity, covering the first 524 bp of its total 796 bp length. The remaining portion of the replicon was not identified in any other contig within the Pm21 assembly or by mapping Illumina reads against its complete coding sequence. This suggests that contig 49 contains a truncated and likely non-functional IncQ1 replicon. BLAST analysis confirmed 100% identity and coverage of contig 49 with the chromosomes of *P. mirabilis* RGF134-1 (CP066833.1) and MPE0346 (CP053719.1), among others. In both animal-origin strains, this sequence is part of a chromosomal multidrug resistance genomic island (GI) containing *sul2*, *aac(3)-IId*, and *aph(6)-Id*, all located within contig 49 (Figure S3).

A bleomycin resistance protein coded by *ble*$_{MBL}$ was identified in contig 53 (6902 bp), downstream the *bla*$_{NDM-5}$ gene. A new assembly performed with plasmidSPAdes resulted in the generation of a longer contig (contig1_PlasmidSPAdes, 8258 bp, https://ri.conicet.gov.ar/handle/11336/252337). This allowed the elucidation of the upstream region of *bla*$_{NDM-5}$, where a truncated sequence of IS*Aba*125 was identified (Figure S4). The *bla*$_{NDM-5}$ genetic context in Pm21 was as follows: (5′–3′: IS*Aba125*, partial sequence - *bla*$_{NDM-5}$ - *ble*$_{MBL}$ - *trpF* - *dsbD* - IS*91* family transposase – *qacEdelta*1 – *sul*1). The IS*91* transposase coding gene was interrupted by IS*Kpn18*, exactly as observed in the IncFIB-IncHI1B plasmids, resulting in the novel genetic platform variant described by González-Espinosa et al. in plasmids pM366-NDM-5 and pM40-NDM-5 (Figure 2) [12].

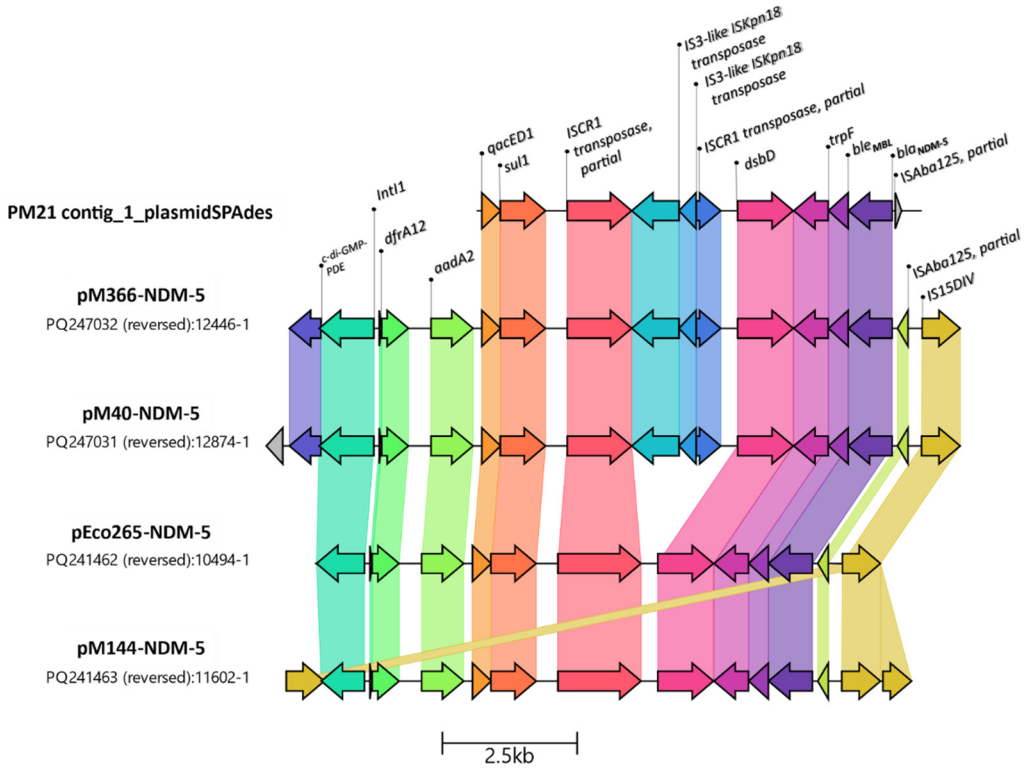

Figure 2. Comparison of the Pm21 contig and its genetic context with IncFII and multi-replicon IncFIB-HI1B plasmids recently reported in Argentina carrying *bla*$_{NDM-5}$. The visualization was generated using Clinker.

BLAST analysis of contig 1_plasmidSPAdes revealed that the top three hits, with 100% coverage and identity, correspond to three *Klebsiella pneumoniae* recently deposited plasmids in Argentina: pM387-NDM5 (accession number CP168953.1), pM40-NDM5 (accession number PQ247031.1), and pM366-NDM5 (accession number PQ247032.1). The last 2 plasmids were fully characterized [12] (https://doi.org/10.1016/j.jgar.2024.10.258). All the remaining 97 hits listed after the BLAST analysis showed 100% identity but only 84% coverage, including *Escherichia coli* strain Ec265 plasmid pEco265-

 doi:10.20944/preprints202504.1221.v1

NDM5 (PQ241462.1) and *K. pneumoniae* plasmid pM144-NDM-5 (PQ241463), which have also been reported in the country (Figure 2).

The whole genome Pm21 assembly was compared to reference sequences using PLSDB with the mash screen search strategy to identify plasmids contained within the sample. The analysis yielded 32 entries, of which 12 contained the *bla*$_{NDM-5}$ gene exclusively in *E. coli*. From these 12 plasmids, only those sequenced both by Illumina and Oxford Nanopore Technologies were further analyzed (10/12) (Table S3). Among the 10 remaining plasmids, 8 had a length of 10,494 bp. BLAST analysis of these plasmids showed 100% coverage and >99.98% similarity among them. Of the remaining two plasmids, one (LC744474.1, 10,687 bp) displayed 95% coverage and >99.98% similarity with the others, while the second plasmid (LC744490.1, 13,652 bp) showed 83% coverage and >99.95% nucleotide similarity (Figure S5). Of the 10 analyzed plasmids, only NZ_CP048374.1, with a length of 10,494 bp, had been previously published in a study assessing the occurrence of carbapenemase-producing *Enterobacteriaceae* (CPE) in freshwater samples from rivers, inland canals, and streams across Switzerland. This plasmid, named pC-F-163_C, was identified in extraintestinal pathogenic *E. coli* ST167, which was nontypeable by incompatibility group [13]. It showed 100% coverage and nucleotide similarity to contig carrying *bla*$_{NDM-5}$ from the Pm21 assembly generated by PlasmidSPAdes.

Additionally, Pm21 strain also harbored the ESBL *bla*$_{CTX-M-15}$ and the 16S ribosomal RNA methyltransferase *rmtB*, which were present in different contigs, 57 (4058 bp) and 67 (1961 bp), respectively. *bla*$_{CTX-M-15}$ was found to have an upstream IS*1380*-like element belonging to the IS*Ecp1* family of transposases, while *rmtB* gene was found in association with two downstream genes encoding a proton antiporter (*cdu2*) and the chaperonin GroEL, identical to other *rmtB*-containing *Enterobacterales* isolates from clinical samples (GenBank accession numbers CP050367, MN061455, MN007141) [11].

2.8. Phylogenetic Tree

To explore ST135 diversity and provide a broader geographic context to Pm21, a core genome SNP phylogenetic tree was generated using all genomic sequences of ST135 *P. mirabilis* available at PubMLST (October 2024). The full dataset containing 123 *P. mirabilis* ST135 isolates is available here: Google Spreadsheet - Proteus mirabilis ST135 dataset). The resulting phylogenetic tree is available at Microreact (https://microreact.org/project/7rKjP28HQQkktYCjLbNbJu-proteuspm21st135). Most isolates are of clinical origin, but some were isolated from food and unknown sources. Besides Pm21, only one isolate carried *bla*$_{NDM-5}$ (ABJNEB000000000.3), which was isolated from a human rectal swab. Our phylogenetic analysis revealed a high degree of dispersion among the *Proteus mirabilis* ST135 isolates. Pm21 did not cluster closely to any of the analyzed genomes. The closest related genome in this analysis was JZ9 which belongs to a Chinese isolate recovered from chicken meat. The prevalence of genes related to bacterial virulence factors including Urease (*ure*C), flagella genes (*flh*A, *fli*F, *fli*G, *fli*P, *fli*L, *flg*N), fimbriae (*mrp*A, *mrp*H, *uca*A, *pmf*A, *pmp*A, *pap*C, *pap*D, *pap*F, *pap*G, *pap*H), hemolysin (*hpm*AB), biofilm formation (*pst*C, *rcs*D), autotransporters (*pta*A, *aip*A), proteases (*zap*A), and siderophore-related (*nrp*R, *ire*A) was greater than 69% in all cases (*nrp*R showed the lowest prevalence 85/123). These results underscore the contribution of virulence determinants to the pathogenicity of ST135 *P. mirabilis*.

3. Discussion

This study documents an outbreak in an Argentine adult hospital attributed to *P. mirabilis* isolates co-producing NDM-5 MBL and CTX-M-15 ESBL. To date, reports of outbreaks caused by MDR *P. mirabilis* are scarce in the literature. Previously documented outbreaks have primarily involved *P. mirabilis* strains harboring carbapenemases such as NDM-1 [14] or VIM-4 [15], as well as ESBLs of the CTX-M-2, VEB-1, and TEM types [16–18].

 doi:10.20944/preprints202504.1221.v1

To our knowledge, this represents the initial documentation of *bla*NDM-5 in *P. mirabilis*, along with the first documented hospital outbreak caused by an NDM-producing *P. mirabilis* strain in Argentina.

Treatment of infections caused by such pathogens is often problematic due to their extensive drug resistance. The resistance pattern observed in these MDR *P. mirabilis* isolates generally reflects the hydrolysis spectrum of NDM-type enzymes, along with the presence of multiple aminoglycoside resistance markers and other antimicrobial resistance genes.

Despite carrying the CTX-M-15 ESBL, these isolates remained susceptible to aztreonam. This antimicrobial agent, together with piperacillin/tazobactam (when feasible), represented one of the few treatment options available for infections caused by this MDR *P. mirabilis* strain during the COVID-19 pandemic, a period marked by significant challenges in patient management.

Since no surveillance cultures were performed on the index case at the time of hospital admission, it was not possible to determine whether this patient introduced the outbreak strain. Moreover, the fact that the first isolate was detected 50 days after hospitalization suggests that the strain was not acquired in the patient's household or workplace but rather within the hospital from an unidentified source. In summary, the absence of surveillance cultures from the index case hampers the ability to trace the outbreak's origins and fully characterize transmission dynamics.

Beyond the appropriate treatment of affected patients, it remains unclear whether infection control measures were reinforced following the outbreak´s detection at the hospital. Given the high transmissibility and persistence of *P. mirabilis* carrying NDM-5, effective infection control strategies are crucial to limiting further dissemination. Our findings suggest that, in line with repetitive sequence-based genomic amplification analyses, MALDI-TOF MS can aid in identifying clonally related groups of the opportunistic pathogen *P. mirabilis*. Supporting our results, previous studies have demonstrated the utility of MALDI-TOF MS as a first-line subtyping tool for the sensitive detection of potential dissemination events in hospital settings involving other opportunistic pathogens, such as *Serratia marcescens*, *Citrobacter freundii* [19] and *Enterobacter* species [20].

As observed in this study, *P. mirabilis* can cause catheter-associated urinary tract infections, largely due to its ability to form biofilms on catheter surfaces [21]. Several strains involved in this outbreak were classified as moderate biofilm producers in vitro. Notably, *P. mirabilis* is among the leading bacterial species responsible for biofilm-related infections associated with medical devices [22].

Interestingly, rifampicin exhibited potential for biofilm disruption at concentrations ≥32 µg/mL, though its clinical efficacy remains uncertain. Nwabor et al. reported that combining rifampicin with carbapenems enhanced antibacterial activity and successfully eradicated established *Acinetobacter baumannii* biofilms [23]. Similarly, Amengol et al. demonstrated that colistin-rifampicin combinations effectively eradicated biofilms of both colistin-resistant and colistin-susceptible *Pseudomonas aeruginosa* [24]. However, to the best of our knowledge, no studies have specifically evaluated the effect of rifampicin on *P. mirabilis* biofilms.

We identified *bla*NDM-5 within a novel variant of the genetic platform recently described on multi-replicon IncFIB-IncHI1B plasmids in *Klebsiella pneumoniae* from Argentina. However, the antimicrobial resistance island containing *bla*NDM-5 in Pm21 could not be linked to any specific plasmid. BLAST analysis revealed no more than 20% of pECO-265-NDM-5 and less than 15% of p366-NDM-5 were covered with Pm21 contigs (Figure S6A,B). pEco265-NDM-5 and pM144-NDM-5 belonged to the IncFII replicon type, encoding a MOB-F relaxase, whereas pM40-NDM-5 and pM366-NDM-5 were associated with multi-replicon IncFIB-IncHI1B plasmids, encoding a MOB-H relaxase [11,12]. Interestingly, neither the IncFII nor the IncHI1B replicons were detected in Pm21; however, the MOB-H relaxase was identified. *bla*NDM-5 has mainly been described in IncX3 plasmids as well as other Inc plasmids such as IncFII and IncI1, and in multi-replicon plasmids [25,26]. These findings indicate limited genetic similarity between circulating local plasmids and Pm21, raising the question of whether small, untypeable plasmids like pC-F-163 have already been circulating and integrating into local genetic platforms. This plasmid was determined to be highly similar at the nucleotide level (99–100%) to plasmids pM309-NDM5 and pM217_FII. Both plasmids were detected in nosocomial *E.*

 doi:10.20944/preprints202504.1221.v1

coli ST167 strains from a hematology ward in Myanmar during 2015–2016 [27]; (GenBank accession numbers AP018833.1 and AP018147.1, respectively). Additionally, pC-F-163_C showed 100% coverage and nucleotide similarity to plasmids circulating in Argentina, as described by González Espinosa et al. [12], including pM144-NDM-5, pEco265-NDM-5, pM40-NDM-5, and pM366-NDM-5, as well as to *bla*$_{NDM-5}$ carrying contig from Pm21 assembly created by PlasmidSPAdes (Figure S7).

Pm21 also harbored the 16S ribosomal RNA methyltransferase *rmtB*, which was present in all plasmids described by González-Espinosa et al., except for pM144-NDM-5. Additionally, *bla*$_{CTX-M-15}$ was detected in Pm21, as well as in the multi-replicon plasmids pM40-NDM-5 and pM366-NDM-5 [12].

The IncQ1 replicon was partially detected at the 5′ end of contig 49. We found that contig 49 had 100% identity and coverage with chromosomal multidrug resistance genomic islands (GI) in *P. mirabilis* of animal origin. According to authors, they found other six similar genomic islands suggesting that the presence and spread of this IncQ1-harboring GI in *P. mirabilis* is not uncommon [28]. Interestingly, a BLAST search using the complete 796 bp *repA* sequence of IncQ1, filtered for *P. mirabilis*, yielded a total of 45 hits. Notably, all sequences with 66% coverage (~529 bp) were found in chromosomal DNA.

Our phylogenetic analysis demonstrated widespread dispersion among the *P. mirabilis* ST135 isolates, suggesting that MLST may not be a highly discriminatory tool for strain differentiation in this species. Given these findings, a more robust approach, such as core genome MLST (cgMLST), may be required for more precise strain typing, as proposed by Chen et al. [29]. However, despite its advantages, cgMLST has not yet been established as a standardized reference method for *P. mirabilis*, unlike in *Klebsiella* spp. This phylogenetic dispersion suggests the emergence of diverse NDM-producing *P. mirabilis* clones, reflecting a growing resistance threat. The global spread of multidrug-resistant strains, first reported in Italy and later in Poland, China, and Japan, underscores the need for effective prevention and control strategies [29].

4. Materials and Methods

4.1. Hospital Setting and Bacterial Isolates

This study was conducted at the Hospital General de Agudos “Carlos G. Durand” in Buenos Aires, Argentina, a 398-bed facility with intensive care units for adults and pediatrics, intermediate care, a coronary unit, and general hospitalization wards. During the COVID-19 pandemic, the government implemented measures to optimize healthcare resources. Patient care was prioritized for SARS-CoV-2-infected individuals, as well as for emergency and critical cases. During periods of high bed occupancy, non-urgent medical interventions were postponed based on medical assessment.

Following the initial detection of carbapenem-resistant *P. mirabilis*, a prospective survey was conducted to identify similar cases. Patient demographic data were saved from the laboratory database.

4.2. Bacterial Identification and Antimicrobial Susceptibility Testing (AST)

Bacterial identification and AST were performed using the MALDI-TOF Vitek-MS® system (bioMérieux, Marcy-l'Étoile, France) and the automated Vitek2 system (bioMérieux), respectively. All AST results were interpreted according to Clinical and Laboratory Standards Institute (CLSI) guidelines [30] at the hospital.

The minimum inhibitory concentration (MIC) of rifampicin was determined using the broth microdilution method in cation-adjusted Mueller–Hinton broth (MHB). Results were interpreted according to the CLSI guidelines [30].

 doi:10.20944/preprints202504.1221.v1

4.3. Resistance Mechanisms

The production of carbapenemases was performed using the diffusion and synergy test with meropenem (MEM) 10 µg and imipenem (IPM) 10 µg discs (Laboratorio Britania, Buenos Aires, Argentina), interspersed with phenylboronic acid (PBA) 300 µg and ethylenediaminetetraacetic acid (EDTA) 1 µmol discs for assessing KPC and MBL, respectively [31].

Genotypic characterization of β-lactamase was carried out at Laboratorio de Resistencia Bacteriana (Facultad de Farmacia y Bioquímica, Universidad de Buenos Aires) using PCR amplification performed on the total DNA using specific primers for detection of metallo-carbapenemases (VIM, IMP and NDM), and extended spectrum β-lactamases (ESBLs) (CTX-M-G1, CTX-M-G2 and CTX-M-G9) and conditions described previously [32,33]. Amplicons were sequenced on both strands using an ABI3730XL DNA Sequencer (Macrogen, Seoul, Republic of Korea).

4.4. Molecular Typing

Clonality of the isolates was determined by the homology relationships among fragments amplified by ERIC-PCR (Enterobacterial Repetitive Intergenic Consensus) and REP-PCR (Repetitive Extragenic Palindromic) according to Versalovic et al. [34].

Cluster analysis was performed using MALDI-TOF MS spectra with at least 110 peaks. A peak range from 3000 to 20000 m/z values was chosen for this clustering. Peaks were defined to be identical by applying a mass accuracy of 0.08% as the SARAMIS standard setting. Spectra were analyzed with a single link agglomerative clustering algorithm, applying the relative taxonomy analysis tool of SARAMIS premium software to show the resulting dendrogram with differences and similarities in relative terms (percent matching masses). As a standard setting, the mass signal intensity was not considered in the cluster analysis [19].

4.5. Biofilm Formation Assays

A crystal violet (CV) assay was performed to evaluate the biofilm-forming ability of *P. mirabilis* isolates from the outbreak, using 96-well tissue-treated microplates [35]. Six isolates were randomly recovered for the assay, originating from different patients and clinical sources: blood culture (three isolates: Pm24, Pm75, and Pm77), tracheal aspirate (Pm27), catheter (Pm64), and urine (Pm21, the sequenced isolate).

Briefly, isolates were subcultured on tryptic soy agar (TSA) for 24 h, and a single colony from each was inoculated into Lysogeny Broth (LB) broth and grown overnight. The cultures were adjusted to a concentration of 10^6 CFU/mL and resuspended in fresh LB. Aliquots (200 µL) of the standardized inoculum were dispensed into sterile, flat-bottom 96-well polystyrene microplates and incubated at 35°C for 48 h. Following incubation, wells were washed with phosphate-buffered saline (PBS) to remove non-adherent cells and stained with 0.01% (w/v) CV for 30 min. The stained biofilms were then washed with distilled water to remove excess dye. To quantify biofilm biomass, the bound CV was solubilized with 95% (v/v) ethanol, and absorbance was measured at 540 nm using a multimode plate reader. Each isolate was tested in octuplicate.

The biofilm-forming ability of the isolates was classified into four categories based on OD values, following Stepanovic et al. [36]:

Non-biofilm formers: $OD \leq ODcut$
Weak biofilm formers: $ODcut < OD \leq 2 \times ODcut$
Moderate biofilm formers: $2 \times ODcut < OD \leq 4 \times ODcut$
Strong biofilm formers: $OD > 4 \times ODcut$

ODcut was defined as the mean OD of the negative control plus its standard deviation.

To assess biofilm formation on a medical device, sections of latex and silicone Foley urinary catheter (2 cm in length) were cut under sterile conditions and incubated statically at 35°C in 4 mL of LB containing 10^6 CFU/mL of the Pm21 isolate. After 24 h, catheter segments were removed, washed

 doi:10.20944/preprints202504.1221.v1

with PBS to eliminate non-adherent bacteria, and stained with CV, as described by Passerini de Rossi et al. (2012) [37]. Stained segments were then visually inspected for biofilm formation.

4.6. Biofilm Antimicrobial Susceptibility

Biofilm susceptibility testing of the Pm21 isolate was performed as described before [35,38], with minor modifications. Briefly, aliquots (150 µL) of the standardized inoculum, as previously described, were added to the wells of a 96-well microplate and incubated at 35°C for 48 h to allow biofilm formation. After incubation, the medium was aseptically removed, wells were washed with PBS, and 200 µL of rifampicin at two-fold serial dilutions (ranging from 256 mg/L to 2 mg/L) prepared in LB was added to the preformed biofilms.

Following overnight incubation, MIC-b was determined as the lowest antibiotic concentration that prevented the establishment of a planktonic bacterial population from the biofilm (i.e., no visible planktonic growth). The antibiotic solutions were then removed, wells were washed, and 200 µL of LB was added. After 24 h of incubation at 35°C, biofilm viability was assessed visually. The minimum re-growth concentration (MRC) was defined as the lowest antibiotic concentration at which bacteria failed to regrow [35,38]. Sterility and antibiotic-free controls were included in all experiments. Each condition was tested in octuplicate.

Additionally, the effect of rifampicin on biofilm biomass was assessed. Biofilms of Pm21 exposed to rifampicin (256 mg/L to 2 mg/L) were stained with CV as previously described. Biomass reduction at each antibiotic concentration (eight wells per dilution) was quantified by calculating the ratio between the OD_{540} values of treated and untreated biofilms.

4.7. Statistical Analysis

Differences in biofilm biomass between untreated and rifampicin-treated samples were assessed using the Kruskal–Wallis test, followed by Dunn's multiple comparison test. All P-values were calculated using one-tailed tests, with a significance level of 0.01. Statistical analyses and graphical representations were performed using GraphPad Software 6.01.

4.8. Whole-Genome Sequencing Analysis

Whole-genome sequencing of *P. mirabilis* Pm21 was performed through short reads on the Illumina NextSeq platform (Department of Microbiology of the Institute of Biomedical Sciences, Universidad de São Paulo, Brazil). Paired-end reads were de novo assembled into contigs using Unicycler (0.5.0+galaxy1) on the Galaxy platform (https://usegalaxy.eu/). Automated annotation was done with Prokka v.1.14.6 and manually curated. The whole-genome shotgun project of *P. mirabilis* Pm21 has been deposited in GenBank (SRA) under accession no. PRJNA1236692. The contig containing *bla*$_{NDM-5}$ (contig 53) was subsequently annotated with BAKTA software (v 1.9.4) [39] to determine its genetic context. A new assembly was performed using plasmidSPAdes (v3.15.5) to obtain a longer contig. Sequence comparisons were performed using BLAST analysis. Strain typing was conducted using the Public Database for Molecular Typing and Microbial Genome Diversity (PubMLST; https://pubmlst.org/organisms/proteus-spp). The resistome was identified through ResFinder (2024-03-22) hosted on the Center for Genomic Epidemiology web page (http://genepi.food.dtu.dk/resfinder). Plasmid detection was carried out with PlasmidFinder v2.0.1, integrated into the staramr tool (v0.11.0) [40]. Additionally, PLSDB, using the Mash screen search strategy, was employed to identify potential plasmid-related sequences and assess their similarity to previously reported plasmids [41–43]. To characterize genomic islands, in silico detection was performed using chromosomes deposited in NCBI and the IslandViewer 4 web server (http://www.pathogenomics.sfu.ca/islandviewer/) [44]. The graphical comparison of genomic islands was visualized with Clinker (https://cagecat.bioinformatics.nl/tools/clinker).

To explore ST135 diversity, a phylogenetic tree was built including Pm21 and all genomic sequences of ST135 *P. mirabilis* available at PubMLST

 doi:10.20944/preprints202504.1221.v1

(https://pubmlst.org/bigsdb?db=pubmlst_proteus_isolates&page=query&genomes=1). Briefly, core genome SNPs for ST135 genomes were determined using snippy (v4.6.0) [45] with the oldest available *P. mirabilis* genome (GB08, GCF_001617295.1) as reference. Recombinant regions were removed using Gubbins (v3.3) [46]. Afterwards, a snp-only alignment was generated from the recombination-free Gubbins output using SNP-sites (v2.5.1) [47], which was used as input for IQ-TREE (v1.6.12) [48]. The tree was built using the best fit model determined with the function '-m TEST' (TVM+F+ASC) and 1000 bootstraps. The tree was visualized with Microreact (https://microreact.org/) [49]. For all ST135 genomes, plasmid replicons, virulence and antimicrobial resistance genes were detected using ABRicate, with different databases and thresholds: PlasmidFinder (default settings); a custom database with *P.mirabilis* virulence-related reference sequences and Virulence Factor Database (VFDB): ID 70%, Coverage 60%; and ResFinder (default settings), respectively.

5. Conclusions

This study highlights the growing threat of NDM-producing *P. mirabilis* in Argentina and underscores the importance of integrating genomic surveillance into infection control protocols to mitigate the spread of MDR pathogens. The dissemination of carbapenemase-producing *Enterobacterales* represents a growing public-health concern. Urgent measures must be taken to promptly identify these isolates within hospital settings and mitigate their spread through stringent infection control protocols. These protocols should encompass active surveillance cultures, segregation or cohorting of carriers, deployment of expert nursing staff, and implementation of proper antimicrobial stewardship initiatives.

Supplementary Materials: The following supporting information can be downloaded at: www.mdpi.com/xxx/s1, Figure S1 to S7 and Table S1 and S2.

Author Contributions: BG: Conceptualization, methodology, data curation, validation, formal analysis, investigation, writing-original draft preparation, writing-review and editing. APR: Conceptualization, methodology, data curation, validation, formal analysis, investigation, writing-review and editing. MSH and LEF: Methodology, data curation, validation, formal analysis, writing-review and editing. NL: Methodology, validation. EO: Conceptualization, data curation, validation, investigation, writing-review and editing. JDC: Conceptualization, methodology, data curation, validation, formal analysis, investigation, resources, writing-original draft preparation, writing-review and editing, supervision, funding acquisition.

Funding: This research was funded by Agencia Nacional de Promoción Científica y Tecnológica (PICT 2019-1879) and UBACyT 2022 (20020220300012BA) to JDC.

Institutional Review Board Statement: The study was conducted in accordance with the Declaration of Helsinki and approved by the Ethics Committee of Facultad de Farmacia y Bioquímica (Universidad de Buenos Aires) for studies involving bacteria recovered from human clinical samples.

Informed Consent Statement: Not applicable.

Data Availability Statement: The whole-genome shotgun project of *P. mirabilis* Pm21 has been deposited in GenBank under the Sequence Read Archive (SRA) accession no. submission: PRJNA1236692. The genome assembly (in Fasta format) used in this paper was deposited in the CONICET Digital Institutional Repository (https://ri.conicet.gov.ar/handle/11336/252337). Other data presented in this study are available upon request from the corresponding author.

Acknowledgments: The authors would like to thank María del Valle Cruz and Florencia Neskovic for their technical support and BRITANIA for the donation of supplies.

Conflicts of Interest: The authors declare no conflicts of interest.

 doi:10.20944/preprints202504.1221.v1

Abbreviations

The following abbreviations are used in this manuscript:

Abbreviation	Meaning
AMK	Amikacin
AST	Antimicrobial Susceptibility Testing
AZT	Aztreonam
CAZ	Ceftazidime
CPE	Carbapenemase-Producing Enterobacteriaceae
CFU	Colony Forming Unit
CIP	Ciprofloxacin
CLSI	Clinical and Laboratory Standards Institute
CTX	Cefotaxime
CV	Crystal Violet
EDTA	Ethylenediaminetetraacetic Acid
ERIC	Enterobacterial Repetitive Intergenic Consensus
ESBL	Extended Spectrum β-lactamase
FEP	Cefepime
GEN	Gentamicin
GI	Genomic Island
IPM	Imipenem
LB	Lysogeny Broth
MALDI-TOF MS	Matrix-Assisted Laser Desorption/Ionization Time-of-Flight Mass Spectrometry
MB	Minimum Biofilm MIC (assumed: MIC-b)
MBL	Metallo-β-lactamase
MDR	Multidrug Resistant
MEM	Meropenem
MIC	Minimum Inhibitory Concentration
MIC-b	Minimum Inhibitory Concentration in the Biofilm Plate
MLST	Multilocus Sequence Typing
MRC	Minimum Re-Growth Concentration
OD	Optical Density
PBA	Phenylboronic Acid
PBS	Phosphate-Buffered Saline
PTZ	Piperacillin/Tazobactam
REP-PCR	Repetitive Extragenic Palindromic PCR
ST	Sequence Type
TMS	Trimethoprim/Sulfamethoxazole
TSA	Tryptic Soy Agar
TSB	Tryptic Soy Broth
WGS	Whole-Genome Sequencing
cgMLST	Core Genome Multilocus Sequence Typing

 doi:10.20944/preprints202504.1221.v1

References

1. Zhu, X.; Zhang, Y.; Shen, Z.; Xia, L.; Wang, J.; Zhao, L.; Wang, K.; Wang, W.; Hao, Z.; Liu, Z. Characterization of NDM-1-Producing Carbapenemase in Proteus Mirabilis among Broilers in China. *Microorganisms* **2021**, *9*, 2443, doi:10.3390/microorganisms9122443.
2. Liu, M.; Li, D.; Jia, W.; Ma, J.; Zhao, X. Study of the Molecular Characteristics and Homology of Carbapenem-Resistant Proteus Mirabilis by Whole Genome Sequencing. *Journal of Medical Microbiology* **2023**, *72*, 001648, doi:10.1099/jmm.0.001648.
3. Bitar, I.; Mattioni Marchetti, V.; Mercato, A.; Nucleo, E.; Anesi, A.; Bracco, S.; Rognoni, V.; Hrabak, J.; Migliavacca, R. Complete Genome and Plasmids Sequences of a Clinical Proteus Mirabilis Isolate Producing Plasmid Mediated NDM-1 From Italy. *Microorganisms* **2020**, *8*, 339, doi:10.3390/microorganisms8030339.
4. Fusco, A.; Coretti, L.; Savio, V.; Buommino, E.; Lembo, F.; Donnarumma, G. Biofilm Formation and Immunomodulatory Activity of Proteus Mirabilis Clinically Isolated Strains. *International Journal of Molecular Sciences* **2017**, *18*, 414, doi:10.3390/ijms18020414.
5. Wilks, S.A.; Fader, M.J.; Keevil, C.W. Novel Insights into the Proteus Mirabilis Crystalline Biofilm Using Real-Time Imaging. *PLOS ONE* **2015**, *10*, e0141711, doi:10.1371/journal.pone.0141711.
6. Ficik, J.; Andrezál, M.; Drahovská, H.; Böhmer, M.; Szemes, T.; Liptáková, A.; Slobodníková, L. Carbapenem-Resistant Klebsiella Pneumoniae in COVID-19 Era—Challenges and Solutions. *Antibiotics* **2023**, *12*, 1285, doi:10.3390/antibiotics12081285.
7. Li, Y.; Yin, M.; Fang, C.; Fu, Y.; Dai, X.; Zeng, W.; Zhang, L. Genetic Analysis of Resistance and Virulence Characteristics of Clinical Multidrug-Resistant Proteus Mirabilis Isolates. *Front. Cell. Infect. Microbiol.* **2023**, *13*, doi:10.3389/fcimb.2023.1229194.
8. Hua, X.; Zhang, L.; Moran, R.A.; Xu, Q.; Sun, L.; Schaik, W. van; Yu, Y. Cointegration as a Mechanism for the Evolution of a KPC-Producing Multidrug Resistance Plasmid in Proteus Mirabilis. *Emerging Microbes & Infections* **2020**.
9. He, J.; Sun, L.; Zhang, L.; Leptihn, S.; Yu, Y.; Hua, X. A Novel SXT/R391 Integrative and Conjugative Element Carries Two Copies of the blaNDM-1 Gene in Proteus Mirabilis. *mSphere* **2021**, *6*, e0058821, doi:10.1128/mSphere.00588-21.
10. Fritzenwanker, M.; Falgenhauer, J.; Hain, T.; Imirzalioglu, C.; Chakraborty, T.; Yao, Y. The Detection of Extensively Drug-Resistant Proteus Mirabilis Strains Harboring Both VIM-4 and VIM-75 Metallo-β-Lactamases from Patients in Germany. *Microorganisms* **2025**, *13*, 266, doi:10.3390/microorganisms13020266.
11. Costa, A.; Figueroa-Espinosa, R.; Gaudenzi, F.; Lincopan, N.; Fuga, B.; Ghiglione, B.; Gutkind, G.; Di Conza, J. Co-Occurrence of NDM-5 and RmtB in a Clinical Isolate of Escherichia Coli Belonging to CC354 in Latin America. *Front. Cell. Infect. Microbiol.* **2021**, *11*, doi:10.3389/fcimb.2021.654852.
12. González-Espinosa, F.; Di Pilato, V.; Calabrese, L.; Costa, E.; Costa, A.; Gutkind, G.; Cejas, D.; Radice, M. Integral Genomic Description of *Bla*NDM-5-Harbouring Plasmids Recovered from *Enterobacterales* in Argentina. *Journal of Global Antimicrobial Resistance* **2024**, *39*, 224–226, doi:10.1016/j.jgar.2024.10.258.
13. Bleichenbacher, S.; Stevens, M.J.A.; Zurfluh, K.; Perreten, V.; Endimiani, A.; Stephan, R.; Nüesch-Inderbinen, M. Environmental Dissemination of Carbapenemase-Producing Enterobacteriaceae in Rivers in Switzerland. *Environmental Pollution* **2020**, *265*, 115081, doi:10.1016/j.envpol.2020.115081.
14. Yang, L.; He, H.; Chen, Q.; Wang, K.; Lin, Y.; Li, P.; Li, J.; Liu, X.; Jia, L.; Song, H.; et al. Nosocomial Outbreak of Carbapenemase-Producing Proteus Mirabilis With Two Novel Salmonella Genomic Island 1 Variants Carrying Different blaNDM–1 Gene Copies in China. *Front. Microbiol.* **2022**, *12*, doi:10.3389/fmicb.2021.800938.
15. Protonotariou, E.; Poulou, A.; Politi, L.; Meletis, G.; Chatzopoulou, F.; Malousi, A.; Metallidis, S.; Tsakris, A.; Skoura, L. Clonal Outbreak Caused by VIM-4-Producing *Proteus Mirabilis* in a Greek Tertiary-Care Hospital. *International Journal of Antimicrobial Agents* **2020**, *56*, 106060, doi:10.1016/j.ijantimicag.2020.106060.
16. Nakano, R.; Nakano, A.; Abe, M.; Inoue, M.; Okamoto, R. Regional Outbreak of CTX-M-2 β-Lactamase-Producing Proteus Mirabilis in Japan. *Journal of Medical Microbiology* **2012**, *61*, 1727–1735, doi:10.1099/jmm.0.049726-0.

 doi:10.20944/preprints202504.1221.v1

17. Cremet, L.; Bemer ,Pascale; Rome ,Joanna; Juvin ,Marie-Emmanuelle; Navas ,Dominique; Bourigault ,Celine; Guillouzouic ,Aurelie; Caroff ,Nathalie; Lepelletier ,Didier; Asseray ,Nathalie; et al. Outbreak Caused by Proteus Mirabilis Isolates Producing Weakly Expressed TEM-Derived Extended-Spectrum β-Lactamase in Spinal Cord Injury Patients with Recurrent Bacteriuria. *Scandinavian Journal of Infectious Diseases* **2011**, *43*, 957–961, doi:10.3109/00365548.2011.601756.
18. Jain, S.; Gaind, R.; Kothari, C.; Sehgal, R.; Shamweel, A.; Thukral, S.S.; Chellani, H.K. VEB-1 Extended-Spectrum β-Lactamase-Producing Multidrug-Resistant Proteus Mirabilis Sepsis Outbreak in a Neonatal Intensive Care Unit in India: Clinical and Diagnostic Implications. *JMM Case Rep* **2016**, *3*, e005056, doi:10.1099/jmmcr.0.005056.
19. Rödel, J.; Mellmann, A.; Stein, C.; Alexi, M.; Kipp, F.; Edel, B.; Dawczynski, K.; Brandt, C.; Seidel, L.; Pfister, W.; et al. Use of MALDI-TOF Mass Spectrometry to Detect Nosocomial Outbreaks of Serratia Marcescens and Citrobacter Freundii. *Eur J Clin Microbiol Infect Dis* **2019**, *38*, 581–591, doi:10.1007/s10096-018-03462-2.
20. De Florio, L.; Riva, E.; Giona, A.; Dedej, E.; Fogolari, M.; Cella, E.; Spoto, S.; Lai, A.; Zehender, G.; Ciccozzi, M.; et al. MALDI-TOF MS Identification and Clustering Applied to Enterobacter Species in Nosocomial Setting. *Front. Microbiol.* **2018**, *9*, doi:10.3389/fmicb.2018.01885.
21. Wasfi, R.; Hamed, S.M.; Amer, M.A.; Fahmy, L.I. Proteus Mirabilis Biofilm: Development and Therapeutic Strategies. *Front Cell Infect Microbiol* **2020**, *10*, 414, doi:10.3389/fcimb.2020.00414.
22. Bouhrour, N.; Nibbering, P.H.; Bendali, F. Medical Device-Associated Biofilm Infections and Multidrug-Resistant Pathogens. *Pathogens* **2024**, *13*, 393, doi:10.3390/pathogens13050393.
23. Nwabor, L.C.; Chukamnerd, A.; Nwabor, O.F.; Pomwised, R.; Voravuthikunchai, S.P.; Chusri, S. Rifampicin Enhanced Carbapenem Activity with Improved Antibacterial Effects and Eradicates Established Acinetobacter Baumannii Biofilms. *Pharmaceuticals* **2023**, *16*, 477, doi:10.3390/ph16040477.
24. Armengol, E.; Kragh, K.N.; Tolker-Nielsen, T.; Sierra, J.M.; Higazy, D.; Ciofu, O.; Viñas, M.; Høiby, N. Colistin Enhances Rifampicin's Antimicrobial Action in Colistin-Resistant Pseudomonas Aeruginosa Biofilms. *Antimicrobial Agents and Chemotherapy* **2023**, *67*, e01641-22, doi:10.1128/aac.01641-22.
25. Marchetti, V.M.; Bitar, I.; Mercato, A.; Nucleo, E.; Bonomini, A.; Pedroni, P.; Hrabak, J.; Migliavacca, R. Complete Nucleotide Sequence of Plasmids of Two Escherichia Coli Strains Carrying blaNDM–5 and blaNDM–5 and blaOXA–181 From the Same Patient. *Front. Microbiol.* **2020**, *10*, doi:10.3389/fmicb.2019.03095.
26. Hornsey, M.; Phee, L.; Wareham, D.W. A Novel Variant, NDM-5, of the New Delhi Metallo-β-Lactamase in a Multidrug-Resistant Escherichia Coli ST648 Isolate Recovered from a Patient in the United Kingdom. *Antimicrob Agents Chemother* **2011**, *55*, 5952–5954, doi:10.1128/AAC.05108-11.
27. Sugawara, Y.; Akeda, Y.; Hagiya, H.; Sakamoto, N.; Takeuchi, D.; Shanmugakani, R.K.; Motooka, D.; Nishi, I.; Zin, K.N.; Aye, M.M.; et al. Spreading Patterns of NDM-Producing Enterobacteriaceae in Clinical and Environmental Settings in Yangon, Myanmar. *Antimicrobial Agents and Chemotherapy* **2019**, *63*, 10.1128/aac.01924-18, doi:10.1128/aac.01924-18.
28. Wang, Q.; Peng, K.; Liu, Y.; Xiao, X.; Wang, Z.; Li, R. Characterization of TMexCD3-TOprJ3, an RND-Type Efflux System Conferring Resistance to Tigecycline in Proteus Mirabilis, and Its Associated Integrative Conjugative Element. *Antimicrobial Agents and Chemotherapy* **2021**, *65*, 10.1128/aac.02712-20, doi:10.1128/aac.02712-20.
29. Chen, S.L.; Kang, Y.T.; Liang, Y.H.; Qiu, X.T.; Li, Z.J. A Core Genome Multilocus Sequence Typing Scheme for Proteus Mirabilis. *Biomed Environ Sci* **2023**, *36*, 343–352, doi:10.3967/bes2023.040.
30. *CLSI M100 Performance Standards for Antimicrobial Susceptibility Testing 30th Edition. CLSI Supplement M100 Clinical and Laboratory Standards Institute; 2020.*;
31. Cordeiro-Moura, J.R.; Fehlberg, L.C.C.; Nodari, C.S.; Matos, A.P. de; Alves, V. de O.; Cayô, R.; Gales, A.C. Performance of Distinct Phenotypic Methods for Carbapenemase Detection: The Influence of Culture Media. *Diagnostic Microbiology and Infectious Disease* **2020**, *96*, 114912, doi:10.1016/j.diagmicrobio.2019.114912.
32. Dominguez, J.E.; Redondo, L.M.; Figueroa Espinosa, R.A.; Cejas, D.; Gutkind, G.O.; Chacana, P.A.; Di Conza, J.A.; Fernández Miyakawa, M.E. Simultaneous Carriage of Mcr-1 and Other Antimicrobial Resistance Determinants in Escherichia Coli From Poultry. *Front Microbiol* **2018**, *9*, 1679, doi:10.3389/fmicb.2018.01679.

 doi:10.20944/preprints202504.1221.v1

33. Marchisio, M.L.; Liebrenz, K.I.; Méndez, E. de los A.; Di Conza, J.A. Molecular Epidemiology of Cefotaxime-Resistant but Ceftazidime-Susceptible Enterobacterales and Evaluation of the in Vitro Bactericidal Activity of Ceftazidime and Cefepime. *Braz J Microbiol* **2021**, *52*, 1853–1863, doi:10.1007/s42770-021-00574-4.
34. Versalovic, J.; Koeuth, T.; Lupski, R. Distribution of Repetitive DNA Sequences in Eubacteria and Application to Finerpriting of Bacterial Enomes. *Nucleic Acids Research* **1991**, *19*, 6823–6831, doi:10.1093/nar/19.24.6823.
35. Passerini de Rossi, B.; García, C.; Calenda, M.; Vay, C.; Franco, M. Activity of Levofloxacin and Ciprofloxacin on Biofilms and Planktonic Cells of Stenotrophomonas Maltophilia Isolates from Patients with Device-Associated Infections. *Int J Antimicrob Agents* **2009**, *34*, 260–264, doi:10.1016/j.ijantimicag.2009.02.022.
36. Stepanovic, S.; Vukovic, D.; Dakic, I.; Savic, B.; Svabic-Vlahovic, M. A Modified Microtiter-Plate Test for Quantification of Staphylococcal Biofilm Formation. *J Microbiol Methods* **2000**, *40*, 175–179, doi:10.1016/s0167-7012(00)00122-6.
37. Passerini de Rossi, B.; Feldman, L.; Pineda, M.S.; Vay, C.; Franco, M. Comparative in Vitro Efficacies of Ethanol-, EDTA- and Levofloxacin-Based Catheter Lock Solutions on Eradication of Stenotrophomonas Maltophilia Biofilms. *J Med Microbiol* **2012**, *61*, 1248–1253, doi:10.1099/jmm.0.039743-0.
38. Cernohorská, L.; Votava, M. Determination of Minimal Regrowth Concentration (MRC) in Clinical Isolates of Various Biofilm-Forming Bacteria. *Folia Microbiol (Praha)* **2004**, *49*, 75–78, doi:10.1007/BF02931650.
39. Schwengers, O.; Jelonek, L.; Dieckmann, M.A.; Beyvers, S.; Blom, J.; Goesmann, A. Bakta: Rapid and Standardized Annotation of Bacterial Genomes via Alignment-Free Sequence Identification. *Microb Genom* **2021**, *7*, 000685, doi:10.1099/mgen.0.000685.
40. Bharat, A.; Petkau, A.; Avery, B.P.; Chen, J.C.; Folster, J.P.; Carson, C.A.; Kearney, A.; Nadon, C.; Mabon, P.; Thiessen, J.; et al. Correlation between Phenotypic and In Silico Detection of Antimicrobial Resistance in Salmonella Enterica in Canada Using Staramr. *Microorganisms* **2022**, *10*, 292, doi:10.3390/microorganisms10020292.
41. Galata, V.; Fehlmann, T.; Backes, C.; Keller, A. PLSDB: A Resource of Complete Bacterial Plasmids. *Nucleic Acids Res* **2019**, *47*, D195–D202, doi:10.1093/nar/gky1050.
42. Molano, L.-A.G.; Hirsch, P.; Hannig, M.; Müller, R.; Keller, A. The PLSDB 2025 Update: Enhanced Annotations and Improved Functionality for Comprehensive Plasmid Research. *Nucleic Acids Res* **2025**, *53*, D189–D196, doi:10.1093/nar/gkae1095.
43. Schmartz, G.P.; Hartung, A.; Hirsch, P.; Kern, F.; Fehlmann, T.; Müller, R.; Keller, A. PLSDB: Advancing a Comprehensive Database of Bacterial Plasmids. *Nucleic Acids Res* **2022**, *50*, D273–D278, doi:10.1093/nar/gkab1111.
44. Siebor, E.; Neuwirth, C. Proteus Genomic Island 1 (PGI1), a New Resistance Genomic Island from Two Proteus Mirabilis French Clinical Isolates. *J Antimicrob Chemother* **2014**, *69*, 3216–3220, doi:10.1093/jac/dku314.
45. Seemann, T. Tseemann/Snippy 2025.
46. Croucher, N.J.; Page, A.J.; Connor, T.R.; Delaney, A.J.; Keane, J.A.; Bentley, S.D.; Parkhill, J.; Harris, S.R. Rapid Phylogenetic Analysis of Large Samples of Recombinant Bacterial Whole Genome Sequences Using Gubbins. *Nucleic Acids Res* **2015**, *43*, e15, doi:10.1093/nar/gku1196.
47. Page, A.J.; Taylor, B.; Delaney, A.J.; Soares, J.; Seemann, T.; Keane, J.A.; Harris, S.R. SNP-Sites: Rapid Efficient Extraction of SNPs from Multi-FASTA Alignments. *Microbial Genomics* **2016**, *2*, e000056, doi:10.1099/mgen.0.000056.

 doi:10.20944/preprints202504.1221.v1

48. Nguyen, L.-T.; Schmidt, H.A.; von Haeseler, A.; Minh, B.Q. IQ-TREE: A Fast and Effective Stochastic Algorithm for Estimating Maximum-Likelihood Phylogenies. *Mol Biol Evol* **2015**, *32*, 268–274, doi:10.1093/molbev/msu300.
49. Argimón, S.; Abudahab, K.; Goater, R.J.E.; Fedosejev, A.; Bhai, J.; Glasner, C.; Feil, E.J.; Holden, M.T.G.; Yeats, C.A.; Grundmann, H.; et al. Microreact: Visualizing and Sharing Data for Genomic Epidemiology and Phylogeography. *Microbial Genomics* **2016**, *2*, e000093, doi:10.1099/mgen.0.000093.